Available online at www.sciencedirect.com

SCIENCE DIRECT

Biochimica et Biophysica Acta 1693 (2004) 101–110

BIOCHIMICA ET BIOPHYSICA ACTA
BBA

www.bba-direct.com

Simultaneous imaging of initiator/effector caspase activity and mitochondrial membrane potential during cell death in living HeLa cells

Hiroshi Kawai[a,*], Takuo Suzuki[a], Tetsu Kobayashi[a], Hiroyuki Mizuguchi[b], Takao Hayakawa[a], Toru Kawanishi[a]

[a] *Division of Biological Chemistry and Biologicals, National Institute of Health Sciences, 1-18-1 Kamiyoga, Setagaya, Tokyo 158-8501, Japan*
[b] *Division of Cellular and Gene Therapy Products, National Institute of Health Sciences, Tokyo 158-8501, Japan*

Received 26 January 2004; received in revised form 19 May 2004; accepted 28 May 2004
Available online 1 July 2004

Abstract

A family of cystein proteases, the caspases, plays a central role in mediating cell death. In this study, we measured the activation of the initiator and effector caspase in real time, and studied the relationship between caspase activity and mitochondrial membrane potential in living cells by means of bioimaging. We also designed and developed a fluorescence resonance energy transfer (FRET)-based genetically encoded fluorescent indicator, which consisted of yellow fluorescent protein (YFP), a peptide sequence which can be cleaved by specific caspases, and cyan fluorescent protein (CFP). Two peptide sequences which could be cleaved by initiator caspases and effector caspases, respectively, were used. Simultaneous real-time measurements of the caspase activity and mitochondrial membrane potential in the cells treated with TNF-α and staurosporine revealed that dying cells showed caspase activation and mitochondrial depolarization, and that these events, however, were not firmly linked. Although it takes anywhere from 1 to over 10 h after the addition of the cell death inducer for the caspases to begin to be activated, initiator caspases and effector caspases are activated within a short period of time at the last stage in the entire process leading to cell death.

Keywords: Cell death; Caspase; Mitochondrial depolarization; Imaging; GFP; Confocal fluorescent microscopy

1. Introduction

Apoptosis is an essential process for excluding damaged or harmful cells and maintaining homeostasis in biological systems. The disruption of this process is assumed to cause various diseases, including cancer, autoimmune diseases, and neurodegenerative diseases. Apoptosis can be induced experimentally by such stimuli as UV irradiation, growth factor withdrawal, death receptor ligands, or cytotoxic drugs. These factors induce cell death via a cascade of protease activation. These proteases are cystein proteases called caspases. They play a central role in the apoptotic cell death machinery [1,2]. Caspases are synthesized as proprotein, which is processed to its matured form and exerts its catalytic activity at the proper time. For a better understanding of cell death and the diseases that result from it, it is important to elucidate the mechanism of caspase activation.

The caspases are divided into two groups, initiator caspases (e.g., caspase-8, -9, -10) and effector caspases (e.g., caspase-3, -6, -7). The initiator caspases act at an earlier stage of cell death, and activate the effector caspases by hydrolytic cleavage [3–9]. The effector caspases cleave various substrates such as lamin, poly(ADP-ribose)polymerase (PARP), and DNA fragmentation factor (DFF), which cause biochemical and morphological changes in cells, and finally bring about cell death [10,11]. For example, tumor necrosis factor (TNF)-α, a well-known apoptosis inducer, activates caspase-8 through signal transduction via the TNF receptor, which is one of the death receptors [3–7,12]. Caspase-8 then cleaves and activates caspase-3, which cleaves various substrates and causes apoptotic cell death.

* Corresponding author. Tel.: +81-3-3700-9084; fax: +81-3-3700-9084.
E-mail address: kawai@nihs.go.jp (H. Kawai).

0167-4889/$ - see front matter © 2004 Elsevier B.V. All rights reserved.
doi:10.1016/j.bbamcr.2004.05.009

However, some cell death inducers, e.g., staurosporine, exert their activity without binding to the death receptor. Mitochondria play a pivotal role in this pathway [8,9,13]. Mitochondrial membranes are affected by the cell death signal, and cytochrome *c* (cyt. *c*) and other apoptosis-related factors are released to cytosol. Cyt. *c* forms a protein complex called apoptosome with Apaf-1 and procaspase-9. Procaspase-9 is processed and activated in apoptosome, and active caspase-9 cleaves caspase-3 to its active form. Previous studies have identified various caspases and revealed their roles in cell death machinery. But how each reaction proceeds, and how these reactions relate to other cellular events during cell death in living cells, has not been thoroughly investigated.

Green fluorescent protein (GFP) and its variants are widely used in biological studies [14]. They are used not only as a fluorescent tag to visualize a certain protein, but also to monitor the dynamic changes of intracellular signals, e.g., Ca^{2+}, IP_3, protein kinase activities, and proteolysis [15–26]. Some of these biological studies used the fluorescent resonance energy transfer (FRET) between cyan fluorescent protein (CFP) and yellow fluorescent protein (YFP) [27]. CFP and YFP were linked with a small peptide and/or functional protein(s), which changed their conformation by means of a certain cellular signal. This conformational change affected the FRET efficiency of the probe, because FRET efficiency relates to the distance and angle between two fluorophores. Since the FRET efficiency can be estimated by the fluorescence ratio of YFP and CFP (YFP/CFP), the change in the intracellular signal can be detected by measuring the CFP and YFP fluorescence. Bioimaging with a fluorescent probe and fluorescence microscopy makes it possible to detect very subtle and rapid signals in living cells, which is otherwise impossible, and to reveal the temporal and spatial relationships between these signals.

Several groups have already developed probes for caspase activity and have monitored the caspase activities in single cells [28–34]. Almost all of these researchers, however, studied only effector caspase or caspase-3. In this study, we tried to monitor the activity of initiator and effector caspases by means of real-time bioimaging, and investigated the relationship among the caspase activation, mitochondrial membrane potential, and morphological changes during cell death. Recently, Ohnuki et al. [32] reported a fluorescent probe for caspase-8, and studied the relationship between caspase-8 activation and β-amyloid toxicity. Takemoto et al. [33] and Luo et al. [34] developed a fluorescent probe for caspase-9 and caspase-8, and carried out real-time imaging. We used a strategy similar to theirs to develop the probe, but our report is the first to show the relationship between initiator caspase activation and mitochondrial depolarization. Because both of these events are important in cell death machinery, clarifying their temporal relationship by simultaneous imaging is a significant step.

2. Materials and methods

2.1. Plasmid construction

Plasmid encoding YFP-CFP was generated by PCR with pECFP-C1 and pEYFP-C1 (Clontech, Palo Alto, CA). The sequence encoding 11 amino acids at the C-terminus of YFP was eliminated in this construct. The linker connecting YFP and CFP was identical with the multi cloning site of pEYFP-C1. This construct was cloned in the *Nhe*I–*Not*I site of pEGFP-N1 vector. The oligonucleotides encoding the respective caspase's substrate sequence were inserted into the *Bsp*EI–*Age*I site, and the oligonucleotide encoding His_{10} followed by a stop codon (TAA) was inserted into the *Bsr*GI–*Not*I site at the C-terminus of CFP. One caspase substrate sequence was derived from procaspase-3 (5′-CCGGACTGGACTGTGGCATTGAGACAGACAGTGGTGTTGATGAA-3′ and 5′-CCGGTTCATCAACACCACTGTCTGTCTCAATGCCACAGTCCAGT-3′), and another was derived from PARP (5′ -CCGGAAAGAGAAAAGGCGATGAGGTGGATGGAGTGGATGAA-3′ and 5′-CCGGTTCATCCACTCCATCCACCTCATCGCCTTTTCTCTTT-3′) [35,36]. The His_{10} sequence was made from the following oligonucleotides, 5′-GTACAAGCACCACCACCACCACCACCACCACCACCACTAAAGC-3′ and 5′-GGCCGCTTTAGTGGTGGTGGTGGTGGTGGTGGTGCTT-3′. The amino acid sequences between YFP and CFP are shown in Fig. 1. Oligonucleotides were provided by Hokkaido System Science Co. (Sapporo, Japan). All cloned sequences were verified by sequencing.

2.2. Cell culture and transfection

HeLa cells were cultured in DMEM (Sigma-Aldrich, St. Louis, MO) supplemented with 100 units/ml of penicillin G, 100 μg/ml of streptomycin and 10% fetal calf serum (GIBCO). Plasmid encoding the fusion protein was transfected into HeLa cells using Effectene Transfection Reagent (QIAGEN, Hilden, Germany) according to the manufacturer's instructions. After 12–24-h incubation with the transfection reagent, the cells were washed with PBS and cultivated on dishes suitable for assay in medium containing 500 μg/ml of G418 for an additional 1–3 days until the assay was performed.

2.3. Extraction and purification of the fusion proteins

Cells expressing the fusion protein were cultured in 60-mm plastic dishes. The cells were washed with PBS and lysed with 20 mM Tris–HCl buffer (pH 7.9) containing 0.5 M NaCl, 5 mM imidazole and 1% Triton X-100. The lysate was centrifuged at $10,000 \times g$ for 10 min at 4 °C and filtered with a 0.45-μm filter. The fusion protein that contained His_{10} was purified with His-Bind Resin (Novagen, Madison, WI) by following the manufacturer's

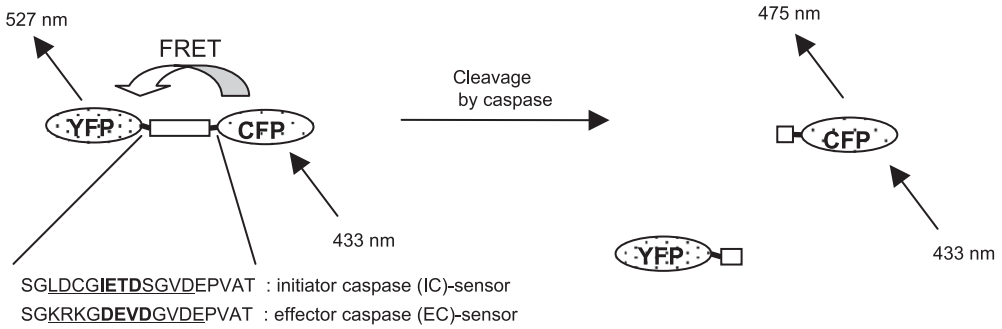

Fig. 1. The probe protein consists of YFP, a substrate peptide of caspase, and CFP. When excited at 433 nm (excitation max. of CFP), this fusion protein shows FRET and emits fluorescence at 527 nm (emission max. of YFP) if the protein is intact. If there are active caspases, the fusion proteins are cleaved, FRET does not occur, and this fusion protein emits fluorescence at 475 nm (emission max. of CFP). The emission ratio of YFP/CFP indicates the caspase activity around the probe protein. The linker region between YFP and CFP consists of 18 amino acids. The sequences derived from procaspase-3 (IC-sensor) and PARP (EC-sensor) are underlined, and the site of consensus recognition by [the] caspase are shown in bold face.

instructions with slight modifications. We used 20 mM imidazole solution instead of 60 mM imidazole solution to wash the resin after loading the sample. Purified fusion proteins were obtained in 20 mM Tris–HCl buffer (pH 7.9) containing 0.5 M NaCl and 1 M imidazole. The solvent was changed to other buffers by centrifugation tube with a MW 30,000 cutoff filter (Millipore, Bedford, MA) if necessary.

2.4. Western blotting

Cells cultured in a plastic dish were washed with PBS and lysed with 1 × SDS loading buffer, or extracted protein sample was mixed with the same amount of 2 × SDS loading buffer. The samples dissolved in 1 × SDS loading buffer were incubated at 95 °C for 2 min, and then they were loaded onto SDS-polyacrylamide gels (10%). Proteins were separated at 20 mA and then blotted to PVDF membranes in Tris–glycine transfer buffer at 100 V for 2 h. The membrane was incubated with block ace (Dainippon Pharmaceutical, Osaka, Japan) for 1 h, anti-GFP monoclonal antibody (Clontech, diluted with 0.1 × block ace to 1:10,000) for 1–2 h, and anti-mouse IgG horseradish peroxidase-conjugated secondary antibody (Chemicon International Inc., Temecula, CA, diluted with 0.1 × block ace to 1:10,000) for 1 h. The membrane was washed with TBS-T two to three times for 5 min after the incubation with the antibody. All of these incubations were performed at room temperature. The membrane was developed with the ECL chemiluminescence detection reagent (Amersham Biosciences, Piscataway, NJ).

2.5. Measurement of fluorescence

The fluorescence of the fusion protein purified by His-Bind Resin was measured using a HITACHI F-310 fluorometer. Fluorescent spectra were scanned from 450 to 550 nm with a scanning speed of 120 nm/min after excitation at 433 nm by Hg lamp.

2.6. Cleavage of the fusion proteins by active caspases

Recombinant human active caspase-1 through caspase-10 were purchased from BioVision (Mountain View, CA). The purified fusion protein dissolved in 1 × Reaction Buffer (BioVision) was incubated with 1 unit of the respective active caspase at 37 °C for 1 h. One unit of the active caspase is the enzyme activity that cleaves 1 nmol of the individual substrate (YVAD-pNA for 1, VDVAD-pNA for 2, DEVD-pNA for 3 and 7, WEHD-pNA for 4 and 5, VEID-pNA for 6, IETD-pNA for 8 and 10, and LEHD-pNA for 9), per hour at 37 °C. Reactions were terminated by adding 2 × SDS loading buffer and subjected to SDS-PAGE and Western blotting.

2.7. Bioimaging with fluorescent microscopy

Transfected cells were cultured on a cover glass (25-mm diameter, 0.15–0.18-mm thickness) for 1–3 days. Cells were treated with TNF-α (200 ng/ml, dissolved in PBS) or staurosporine (3 μM, dissolved in DMSO), and then incubated under the usual culture condition for 1–2 h before analysis. Tetramethylrhodamine methyl ester (TMRM, 50 nM, dissolved in DMSO) was added 20–30 min before the analysis if mitochondrial membrane potential was to be measured. Analyses were carried out by confocal laser scanning fluorescent microscopy using a Carl Zeiss LSM510 system. During the observation, the media were buffered with 10 mM HEPES buffer (pH 7.4) and the cells were maintained at 35–37 °C. DIC images and grayscale images for fluorescence channels were obtained every 2 min unless otherwise described. Excitation lights for the FRET probe (458 nm) and TMRM (543 nm) were provided by an Ar laser with a 458 dichroic mirror and a HeNe laser with a 543 dichroic mirror, respectively. Images of the FRET probe were obtained separately for both cyan and yellow fluorescence using a 515 dichroic mirror and a BP467.5–497.5 emission filter for the cyan and a BP515–545 emission filter for the yellow. Images of TMRM were obtained using a

LP560 emission filter. At first, we tried a BP475–515 filter and a LP515 filter, which were loaded as a standard set in LSM510, for cyan and yellow fluorescence, respectively, but this setting was not suitable for our experiments for several reasons. First, the cyan fluorescence obtained through the BP475–515 filter was too weak, and second the LP515 filter cannot exclude the possibility that TMRM-derived fluorescence contaminated the channel for yellow fluorescence. We prepared several emission filters, and obtained the best results using the setting described above. Contamination of the fluorescence between the channels was negligible in this condition (data not shown). Images were processed and quantified using MetaFluor software. The fluorescent intensity of the whole cell area was used in this analysis. As cells changed their morphology during the observation, the whole cell areas were determined separately in each image.

3. Results

3.1. Design of the probes

We designed and developed a FRET-based genetically encoded fluorescent indicator, which consisted of YFP, a peptide sequence which can be cleaved by specific caspases, and CFP. Since FRET efficiency depends on the distance between CFP and YFP, this fusion protein should show FRET, which can be significantly reduced when the peptide sequence is cleaved by active caspases (Fig. 1). We used two peptide sequences, which were 12 amino acids in length and contained a caspase recognition site in the middle. One was derived from procaspase-3, and was expected to be cleaved by caspase-8/9/10, and the other was from PARP, and was expected to be cleaved by caspase-3/6/7. These probes, which we named the initiator caspase (IC)-sensor and effector caspase (EC)-sensor, were able to indicate the cleavage of procaspase-3 and PARP; in other words, they were able to indicate the protease activities of the initiator caspases and effector caspases, respectively.

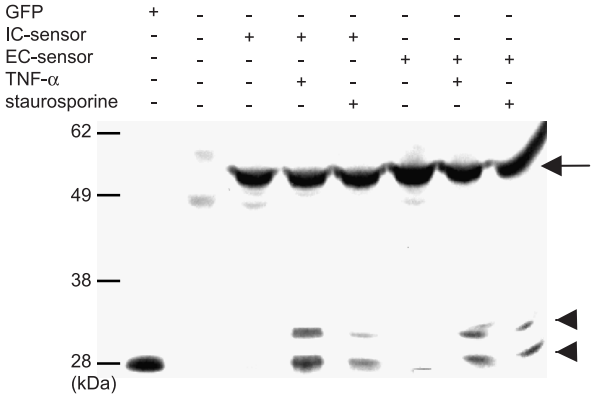

Fig. 2. Expression and cleavage of the probe proteins in HeLa cells. HeLa cells transfected with plasmid encoding IC-sensor (lanes 3–5) or EC-sensor (lanes 6–8) were exposed with 200 ng/ml of TNF-α (lanes 4 and 7) or 3 μM of staurosporine (lanes 5 and 8) for 6 h. The cell lysate of each experiment was prepared and analyzed by Western blot analysis with anti-GFP monoclonal antibody. A control experiment (non-transfected, non-treated HeLa cells, lane 2) shows no band. Lane 1 shows recombinant GFP as a reference. The arrow and arrowheads indicate intact and cleaved YFP-peptide-CFP, respectively.

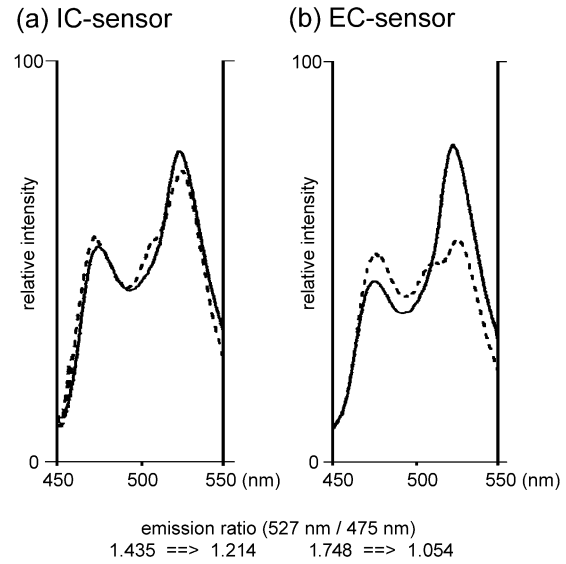

Fig. 3. The fluorescent changes by the cell death stimuli. HeLa cells expressing the IC-sensor or EC-sensor were incubated in the presence or absence of 200 ng/ml of TNF-α for 6 h. The probe protein was extracted and purified as described in Section 2, and the fluorescent spectra with excitation at 433 nm were measured. The fluorescent spectra of the IC-sensor (a) and EC-sensor (b) from non-treated cells (solid line) and TNF-α-treated cells (dotted line) are shown.

3.2. Characterization of the probe proteins in living cells

HeLa cells expressing one of the probe proteins were treated with a cell death inducer, consisting of either 200 ng/ml of TNF-α or 3 μM of staurosporine. After 6 h of exposure, the cells were lysed and underwent Western blot analysis. As shown in Fig. 2, both probe proteins were detected from the transfected HeLa cells (lanes 3–8), and the 25–30-kDa fragments were detected from the cells treated with TNF-α (lanes 4 and 7) or staurosporine (lanes 5 and 8). These fragments were identical to the cleaved fragments (YFP-cleaved peptide and cleaved peptide-CFP-His_{10}). Both the IC-sensor and EC-sensor are successfully expressed in HeLa cells, and are cleaved in cells by cell death stimuli.

The fluorescent spectra of the probe proteins were measured after purification with a His tag. Fig. 3 shows the fluorescent spectra of the IC-sensor (a) and EC-sensor (b) from the TNF-α-treated and non-treated (control) HeLa cells expressing one of the probe proteins. The probe proteins from the control cells showed spectra with two emission peaks at 475 and 527 nm by excitation at 433 nm

(solid line in Fig. 3(a) and (b)). These peaks were identical to those of CFP and YFP, respectively. The probe protein from the TNF-α-treated cells also showed spectra with two peaks, but compared with the non-treated control, the emission at 475 nm was enhanced, and that at 527 nm was reduced (dotted line in Fig. 3(a) and (b)). This result is likely due to the cleavage of the probe protein by caspases, which reduce the energy transfer from CFP to YFP. The ratio of the emission intensity (527/475 nm) was reduced by about 20–40% by the TNF-α treatment in this assay. The staurosporine treatment produced the same results as the TNF-α treatment (data not shown).

YFP can be excited directly by excitation light at 433 nm, and, therefore, YFP fluorescence itself is not an indicator for FRET. We measured the fluorescent ratio, and showed that the ratio was reduced by cell death stimuli, indicating that FRET from CFP to YFP was reduced. The fluorescent ratio can be an indicator for FRET, and the reduction of the ratio indicates the activation of the caspases. We used the fluorescent ratio as the indicator for caspase activation in the following experiments.

3.3. Cleavage of the fusion protein by recombinant caspase

In a cell-free system, we investigated which caspase could cleave IC- and EC-sensors to confirm the specificity of the probe proteins. The probe protein purified from a HeLa cell lysate was incubated with human recombinant caspase-1–10, and Western blotting with an anti-GFP antibody was used to confirm whether the probe protein was cleaved by the respective caspases. Fig. 4 shows the results. The IC-sensor was cleaved by caspase-8 and caspase-9, and slightly by caspase-5 and caspase-6. The bands for the cleaved probe proteins were quantified, and the activities of caspase-8 and -9 were estimated to be 5–10 times higher than that of caspase-5 and -6. The EC-sensor was cleaved by caspase-3, and slightly by caspase-7, -8, and -9. The caspase-3 activity was more than 10 times higher than the activity of the other caspases. Although we cannot exclude the possibility that some caspases can cleave the probes in living cells despite their inability to cleave them in this cell-free system, or that some proteases other than caspase-1–10 can cleave them, these results clearly showed that the IC- and EC-sensor proteins could mainly detect the caspase-8/9 activity and caspase-3 activity, respectively.

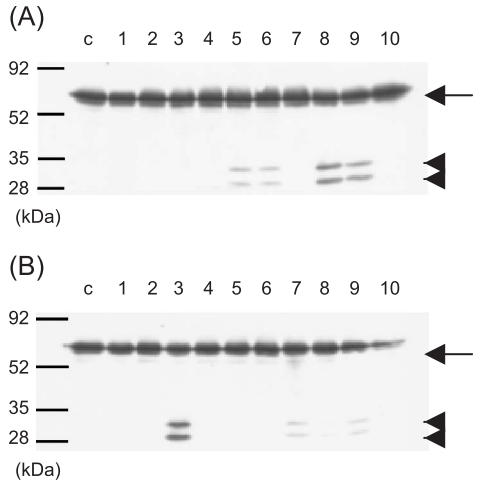

Fig. 4. Selective cleavage of the probe proteins by certain caspases. The probe protein was incubated with recombinant active caspase-1–10 at 37 C for 1 h. The resultants were analyzed by Western blotting with anti-GFP monoclonal antibody. (A) IC-sensor; (B) EC-sensor. Numbers 1–10 represent the results from assays with caspase-1–10, respectively, and c represents the control experiment in which the assay was performed in the absence of caspase. The arrow and arrowheads indicate intact and cleaved sensor proteins, respectively.

3.4. Simultaneous bioimaging of caspase activity and mitochondrial membrane potential

Next, we tried to carry out real-time detection of the caspase activity and mitochondrial membrane potential in single living cells. HeLa cells were transfected with the caspase-sensor and treated with 50 nM of TMRM, a mitochondrial membrane potential-indicator. It has been reported that TMRM is less toxic than tetramethylrhodamine ethyl ester, and does not inhibit mitochondrial respiration at this dose [37]. The caspase activity and mitochondrial membrane potential were simultaneously measured in living cells every 2 min by confocal laser-scanning fluorescent microscopy, as described in Section 2. A control study in which the cells were treated with solvent (DMSO, 1%) did not show any fluorescent or morphological changes (data not shown).

Fig. 5 shows typical images of the assay. Cells expressing the IC-sensor were treated with 200 ng/ml of TNF-α (a) or 3 μM of staurosporine (b). After 1–6-h exposure, changes were observed in some cells. The fluorescence of the CFP channel increased, while that of the YFP channel decreased (not shown in Fig. 5; see Fig. 6), and the emission ratio of YFP/CFP, which represents the FRET efficiency, dramatically decreased, indicating that the caspases were activated. The fluorescence of TMRM also decreased, indicating that the mitochondrial membrane potential was reduced. As previously reported by other groups, the timing of the response differs in each cell [28–30,33,34]. Since several reports suggested that the induction of apoptosis is related to the cell cycle, the difference of timing we observed here might depend on which cell-cycle phase the individual cells were in [38,39].

3.5. Morphology during cell death induced by TNF-α or staurosporine

There were differences in morphology between the TNF-α-treated and staurosporine-treated cells. The TNF-α-treated cells shrank drastically when the caspase was activated, whereas the staurosporine-treated cells did not show such obvious changes in morphology, although the caspases were

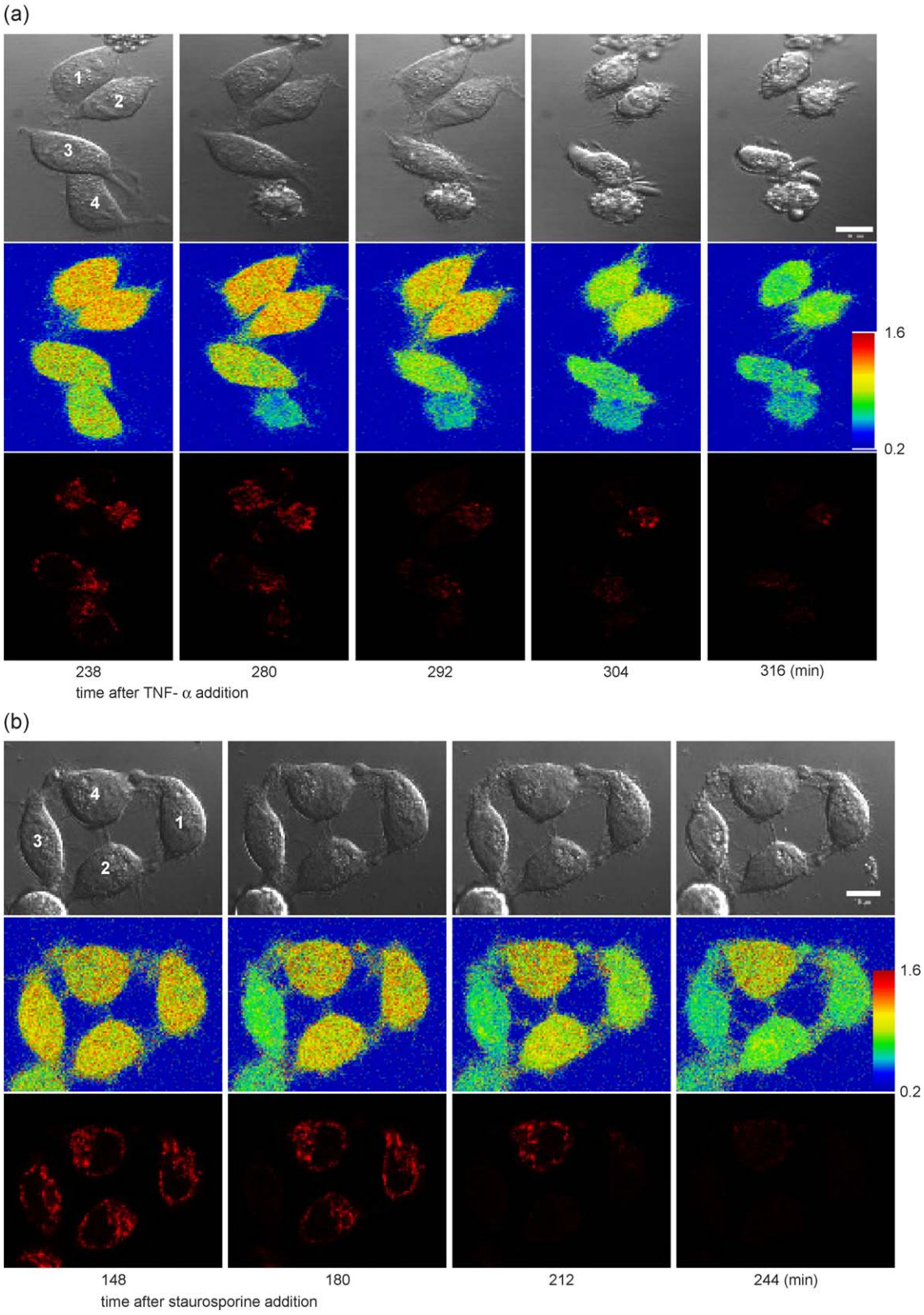

Fig. 5. Time lapse images of the caspase activity and the mitochondrial membrane potential obtained by LSM510. HeLa cells expressing the IC-sensor were incubated with 200 ng/ml of TNF-α (a) or 3 μM of staurosporine (b). The cells were then observed by confocal microscopy, and DIC and fluorescent images were obtained at 2-min intervals, as described in Section 2. DIC images (upper panels), the emission ratio of YFP/CFP (middle panels), and the fluorescent intensity of TMRM (lower panels) at the indicated time are shown in pseudo colors. The reduction of the YFP/CFP ratio represents caspase activation, and the reduction of TMRM fluorescence represents the reduction of the mitochondrial membrane potential. The bars in the upper right images indicate 10 μm.

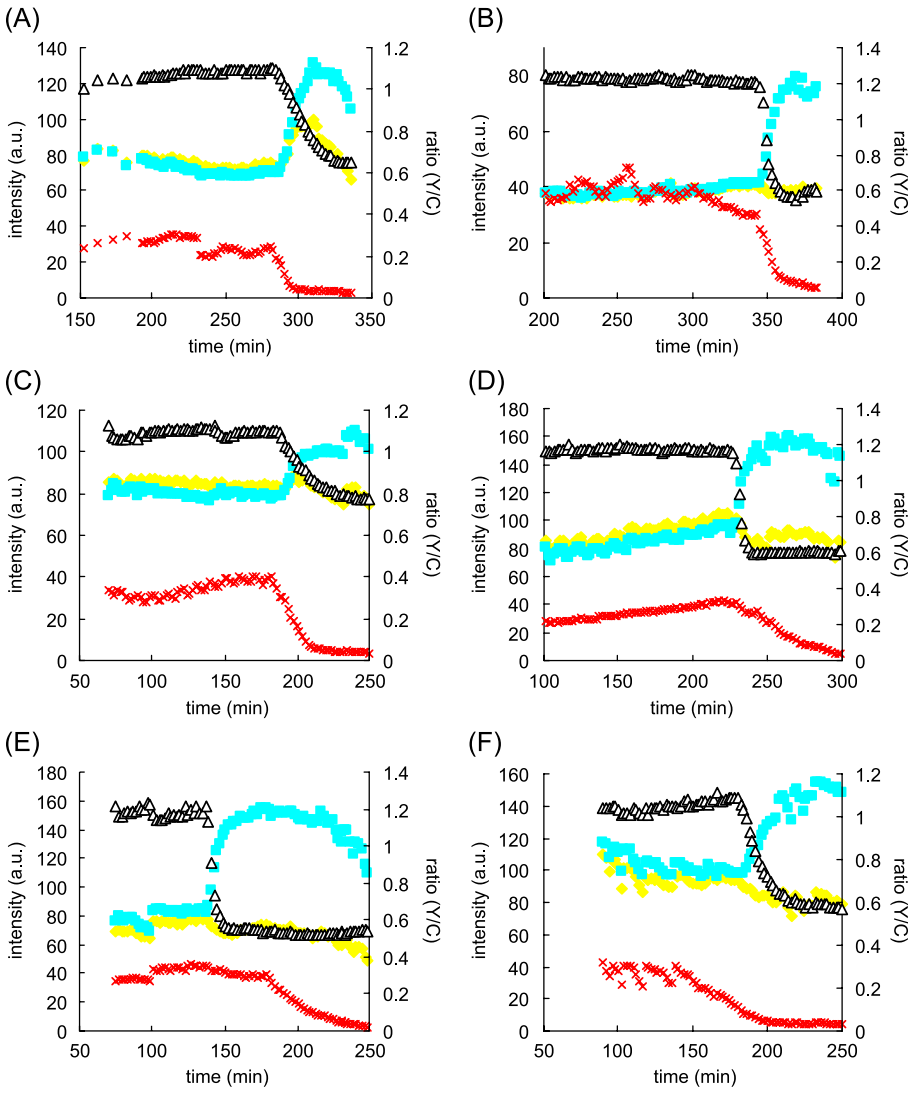

Fig. 6. Fluorescent changes during cell death. HeLa cells expressing the IC-sensor (A, C) or EC-sensor (B, D, E, F) were incubated with 200 ng/ml of TNF-α (A, B) or 3 μM of staurosporine (C, D, E, F). Fluorescent images as shown in Fig. 5 were obtained from each experiment, and then the YFP/CFP ratio and the fluorescence of CFP, YFP, and TMRM for the whole single cell area were quantified and plotted. A–D each show a representative example of each treatment. Filled square (cyan): CFP; filled diamond (yellow): YFP; open triangle: ratio (YFP/CFP); ×: TMRM (red). The vertical axes show the mean pixel intensity of the whole cell region (left; CFP, YFP, and TMRM) and the mean pixel emission ratio of the whole cell region (right; YFP/CFP ratio). a.u., arbitrary units.

activated and the mitochondrial membrane potential reduced, just as in the TNF-α-treated cells (Fig. 5). The temporal relationship between the caspase activation and the morphological changes probably differs in these two treatments. We speculated that other factor(s) are necessary for the morphological changes during cell death to occur, and that these factors are activated almost simultaneously with the caspase in TNF-α-treated cells, whereas it takes time to activate them after the caspase activation in staurosporine-treated cells.

3.6. Temporal relationship of caspase activation and mitochondrial depolarization

Fig. 6(A)–(D) shows typical examples of the fluorescent changes that occurred in each treatment. The fluorescent intensity of the caspase-sensor and TMRM, and the ratio of the YFP and CFP fluorescence of the caspase-sensor were plotted. The horizontal axes indicate the time after the cell death-inducer treatment. Each graph shows the results from a respective single cell. (A) and (C) show the results from cell #1 in Fig. 5(a) and (b), respectively. The emission ratio of YFP/CFP was dramatically reduced, indicating that the caspase was activated at this point in that cell. The fluorescence intensity of TMRM was reduced, indicating that the mitochondria depolarized at this point in that cell. Fig. 6(E) and (F) shows examples with a large time difference between the caspase activation and the mitochondrial depolarization. Caspase activation was observed 44 min earlier than the mitochondrial depolarization in the cell shown in Fig. 6(E), whereas caspase activation was observed 42 min

later than the mitochondrial depolarization in the cell shown in Fig. 6(F).

The YFP emission should have decreased with the caspase activation in ideal FRET system. However, the YFP emission remained constant or increased in some cases (Fig. 6). We considered this to have occurred because the cells shrank immediately after caspase activation, especially in the TNF-α-induced cell death, as shown in Fig. 5. This caused the concentration of the fluorescent protein in the cell, resulting in an increase of the CFP and YFP signals in the confocal slice. This concentration effect was cancelled out by ratiometric analysis. YFP showed unexpected fluorescent changes in some cases, but we were able to evaluate the FRET change properly by analyzing the fluorescent ratio of YFP and CFP.

Sensor proteins were transiently transfected, and the concentration of the sensor proteins was shown to be different in each cell. Some cells expressed a high level of sensor proteins and showed bright fluorescence, and other cells expressed a low level of sensor proteins and showed dim fluorescence. However, we found that the expression level of the sensor proteins did not affect the slope of the ratio trace.

In order to study the temporal relationship between the caspase activation and the mitochondrial depolarization, we carried out a quantitative analysis and estimated the relative timing of the initiator- and effector-caspase activation and mitochondrial depolarization. The starting point of the reduction of the YFP/CFP ratio (A, indicated by an arrow in Fig. 7(a)) and that of the TMRM fluorescence (B, indicated by an arrowhead in Fig. 7(a)) were determined as the time point after which the value decreased during four continuous points or more, the value decreased more than 20% in total, and the reduction of the value was the last one in the experiment. We determined these points in each cell, and calculated the time interval from B to A. We analyzed 31–47 cells in at least seven independent experiments for each treatment, and plotted the results in Fig. 7(b). Here, each plot represents the result from a cell, with time 0 being the point at which the TMRM fluorescence started to decrease. If the plot is on −10, for example, this means that the caspase activation occurred 10 min earlier than the mitochondrial depolarization in that cell. This analysis clarified the temporal relationship between mitochondrial depolarization, initiator caspase activation, and effector caspase activation.

Although Fig. 7 shows some scatter, which suggest that the relationship between caspase activation and mitochondrial depolarization is not firm, we can estimate the relationship between the two by quantitative analysis. A trend was seen in which the median values and mean values of the time interval were estimated to be nearly 0 in all treatments. This means that the caspase activation and mitochondrial depolarization are likely to start within a short amount of time in the majority of cells, compared with the duration from drug treatment to these events, which takes anywhere

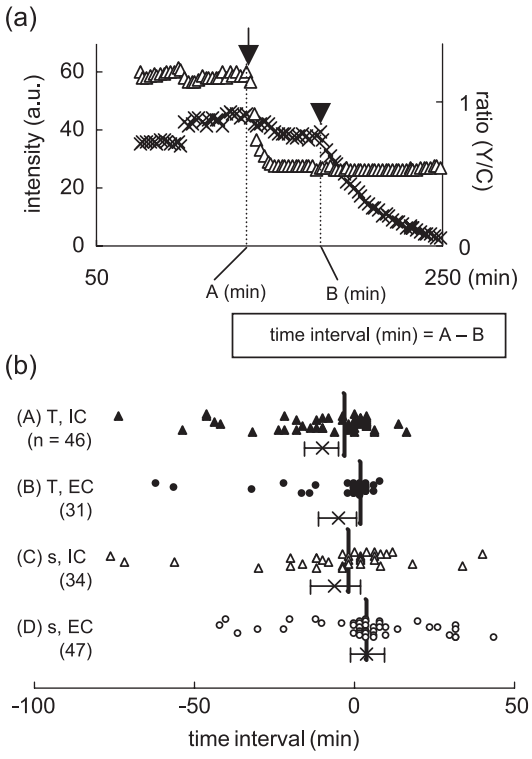

Fig. 7. The time intervals between mitochondrial depolarization and caspase activation. (a) We defined the difference between the two time points indicated by the arrow and arrowhead as the time interval. Details are described in the text. (b) We calculated and plotted this parameter for each cell. Each plot represents one cell. The vertical lines, crosses, and bars represent the median, mean, and 95% confidence interval for each group. The number of cells used in each analysis is shown in parenthesis. Filled mark (A, B): TNF-α; open mark (C, D): staurosporine; triangle (A, C): IC-sensor; circle (B, D): EC-sensor.

from 1 to over 10 h. Because initiator caspases are proteases that cleave and activate effector caspases, the initiator caspase might be activated earlier than the effector caspase. Our results suggest that the effector caspase activation occurred immediately after the initiator caspase activation.

4. Discussion

In this study, we described a method for measuring changes in the initiator or effector caspase activity and mitochondrial membrane potential simultaneously in single living cells in real time by means of bioimaging, which revealed the kinetics of the caspase activation and the relationship among the caspase activities, mitochondrial membrane potential, and morphological changes during cell death. The time schedule of cell death is different in each cell, but dying cells show caspase activation and a reduction of the mitochondrial membrane potential. In a dying cell, it takes a long time, 1–10 h or more, from the addition of cell death-inducers to start initiator caspase activation, and it takes a relatively short time from the initiator caspase activation to start effector caspase activation. This finding

suggests that the caspase cascade proceeds within a short amount of time at the last stage in the entire biochemical process leading to cell death.

Luo et al. [34] reported that the activation of caspase-8 occurred much earlier than that of caspase-3 in TNF-α-induced apoptosis. They calculated the time difference between these activations as about 120 min on average, which differed from ours. They measured the timing of the caspase activation by comparing it with the timing of the morphological change, which is very difficult to determine. In our experiments, we compared the timing of the caspase activation with that of mitochondrial depolarization, which is much easier to analyze objectively, especially in the case of staurosporine-induced cell death, which showed little morphological change (Fig. 5). Therefore, we feel that our conclusion is more reliable.

It is widely accepted that TNF-α brings about cell death via binding with its receptor, receptor trimerization, binding of the intracellular domain of the receptor with adaptor proteins, cleavage (activation) of the initiator caspase (caspase-8), and cleavage (activation) of the effector caspase (caspase-3) [1]. In this study, we investigated the time course of this pathway, and revealed that it takes a long time after drug treatment, more than 10 h in some cases, to start caspase activation. We speculate that this is a period in which initiator caspase activation is prepared for. There are likely some unknown factors which are essential to activating the initiator caspases. These factors delay the cell death process and they determine the timing of cell death. Once these events occur, the activation of caspases and further cell death processes may proceed immediately.

The wide distribution of the plots in Fig. 7 suggests that caspase activation and mitochondrial depolarization are not firmly linked. Some cells showed mitochondrial depolarization earlier than caspase activation, and the other cells showed mitochondrial depolarization later than caspase activation, suggesting that these two events are independently induced in cell death machinery. When cell death is induced via mitochondrial change, cyt. *c* is released from the mitochondria to the cytosol, which is a critical event for cell death [1,8,9]. Cyt. *c* release leads caspase activation by the formation of apoptosome in the cytosol. Both caspase activation and mitochondrial depolarization relate to mitochondrial change, so these reactions occur within a short amount of time in the majority of cells. But these reactions occur with a large time interval in some cells because their relationship is indirect and not rigid. The time schedule of the process leading to each event may respectively depend on individual cellular conditions. Luetjens et al. [40] have reported on the mode of cyt. *c* release, and showed that cyt. *c* was released within 10 min in the majority of cells, whereas cyt. *c* was released stepwise with an intermediate plateau about 30 min in duration in 13% of the release events they observed. In some cells, a certain amount of cyt. *c* was released from the mitochondria to cytosol, which was enough to cause the apoptosome formation and the following caspase activation, but not enough to cause the mitochondrial depolarization because the cyt. *c* remaining in the mitochondria can maintain the membrane potential. Early caspase activation and late mitochondrial depolarization would be observed in this case.

Cyt. *c* release and mitochondrial depolarization have been analyzed using GFP-tagged cyt. *c* and potentiometric dye such as TMRM [41]. It is likely that mitochondrial depolarization is not required and is not sufficient for cyt. *c* release [42], but the temporal relationship between cyt. *c* release and depolarization is still controversial. Some researchers have showed that cyt. *c* was released a long time before mitochondrial depolarization [43,44], whereas others have reported that cyt. *c* release followed mitochondrial depolarization [45]. The timing of mitochondrial depolarization seems to depend on various factors, including the cell death stimulant, cell type, and individual cell condition. The relationship between caspase activation and mitochondrial changes (cyt. *c* release, depolarization) needs to be studied further.

Acknowledgements

This study was supported in part by a grant-in-aid for the Research on Health Sciences focusing on Drug Innovation from the Japan Health Science Foundation, a grant-in-aid for the Research on Advanced Medical Technology from Ministry of Health Labour and Welfare, a grant (MF-16) from the Organization for Pharmaceutical Safety and Research.

References

[1] N.A. Thornberry, Y. Lazebnik, Caspases: enemies within, Science 281 (1998) 1312–1316.
[2] H.R. Stennicke, G.S. Salvesen, Properties of caspases, Biochim. Biophys. Acta 1387 (1998) 17–31.
[3] M.P. Boldin, T.M. Goncharov, Y.V. Goltsev, D. Wallach, Involvement of MACH, a novel MORT1/FADD-interacting protease, in Fas/APO-1- and TNF receptor-induced cell death, Cell 85 (1996) 803–815.
[4] M. Muzio, A.M. Chinnaiyan, F.C. Kischkell, K. O'Rourke, A. Shevchenko, J. Ni, C. Scaffidi, J.D. Bretz, M. Zhang, R. Gentz, M. Mann, P.H. Krammer, M.E. Peter, V.M. Dixit, FLICE, a novel FADD-homologous ICE/CED-3-like protease, is recruited to the CD95 (Fas/APO-1) death-inducing signal complex, Cell 85 (1996) 817–827.
[5] J.P. Medema, C. Scaffidi, F.C. Kischkel, A. Shevchenko, M. Mann, P.H. Krammer, M.E. Peter, FLICE is activated by association with the CD95 death-inducing signaling complex (DISC), EMBO J. 16 (1997) 2794–2804.
[6] D.A. Martin, R.M. Siegel, L. Zheng, M.J. Lenardo, Membrane oligomerization and cleavage activates the caspase-8 (FLICE/MACHα1) death signal, J. Biol. Chem. 273 (1998) 4345–4349.
[7] S.M. Srinivasula, M. Ahmad, T. Fernandes-Alnemri, G. Litwack, E.S. Alnemri, Molecular ordering of the Fas-apoptotic pathway: the Fas/APO-1 protease Mch5 is a CrmA-inhibitable protease that activates multiple Ced-3/ICE-like cysteine proteases, Proc. Natl. Acad. Sci. U. S. A. 93 (1996) 14486–14491.

[8] A. Saleh, S.M. Srinivasula, S. Acharya, R. Fishel, E.S. Alnemri, Cytochrome *c* and dATP-mediated oligomerization of Apaf-1 is a prerequisite for procaspase-9 activation, J. Biol. Chem. 274 (1999) 17941–17945.
[9] E.N. Shiozaki, J. Chai, Y. Shi, Oligomerization and activation of caspase-9, induced by Apaf-1 CARD, Proc. Natl. Acad. Sci. U. S. A. 99 (2002) 4197–4202.
[10] K. Orth, K. O'Rourke, G.S. Salvesen, V.M. Dixit, Molecular ordering of apoptotic mammalian CED-3/ICE-like proteases, J. Biol. Chem. 271 (1996) 20977–20980.
[11] M. Tewari, L.T. Quan, K. O'Rourke, S. Desnoyers, Z. Zeng, D.R. Beidler, G.G. Poirier, G.S. Salvesen, V.M. Dixit, Yama/CPP32β, a mammalian homolog of CED-3, is a CrmA-inhibitable protease that cleaves the death substrate poly(ADP-ribose) polymerase, Cell 81 (1995) 801–809.
[12] A. Ashkenazi, V.M. Dixit, Death receptors: signaling and modulation, Science 281 (1998) 1305–1308.
[13] D.R. Green, J.C. Reed, Mitochondria and apoptosis, Science 281 (1998) 1309–1312.
[14] R.Y. Tsien, The green fluorescent protein, Annu. Rev. Biochem. 67 (1998) 509–544.
[15] A. Miyawaki, J. Llopis, R. Heim, J.M. Mccaffery, J.A. Adams, M. Ikura, R.Y. Tsien, Fluorescent indicators for Ca^{2+} based on green fluorescent proteins and calmodulin, Nature 388 (1997) 882–887.
[16] K. Hirose, S. Kadowaki, M. Tanabe, H. Takeshima, M. Iino, Spatiotemporal dynamics of inositol 1,4,5-trisphosphate that underlies complex Ca^{2+} mobilization patterns, Science 284 (1999) 1527–1530.
[17] M. Zaccolo, F.D. Giorgi, C.Y. Cho, L. Feng, T. Knapp, P.A. Negulescu, S.S. Taylor, R.Y. Tsien, T. Pozzan, A genetically encoded, fluorescent indicator for cyclic AMP in living cells, Nat. Cell Biol. 2 (2000) 25–29.
[18] Y. Nagai, M. Miyazaki, R. Aoki, T. Zama, S. Inouye, K. Hirose, M. Iino, M. Hagiwara, A fluorescent indicator for visualizing cAMP-induced phosphorylation in vivo, Nat. Biotech. 18 (2000) 313–316.
[19] N.P. Dantuma, K. Lindsten, R. Glas, M. Jellne, M.G. Masucci, Short-lived green fluorescent proteins for quantifying ubiquitin/proteasome-dependent proteolysis in living cells, Nat. Biotechnol. 18 (2000) 538–543.
[20] M. Sato, N. Hida, T. Ozawa, Y. Umezawa, Fluorescent indicators for cyclic GMP based on cyclic GMP-dependent protein kinase Iα and green fluorescent proteins, Anal. Chem. 72 (2000) 5918–5924.
[21] T. Nagai, A. Sawano, E.S. Park, A. Miyawaki, Circularly permuted green fluorescent proteins engineered to sense Ca^{2+}, Proc. Natl. Acad. Sci. U. S. A. 98 (2001) 3197–3202.
[22] K. Kurokawa, N. Mochizuki, Y. Ohba, H. Mizuno, A. Miyawaki, M. Matsuda, A pair of fluorescent resonance energy transfer-based probes for tyrosine phosphorylation of the CrkII adaptor protein in vivo, J. Biol. Chem. 276 (2001) 31305–31310.
[23] J. Zhang, Y. Ma, S.S. Taylor, R.Y. Tsien, Genetically encoded reporters of proein kinase A activity reveal impact of substrate tethering, Proc. Natl. Acad. Sci. U. S. A. 98 (2001) 14997–15002.
[24] A.Y. Ting, K.H. Kain, R.L. Klemke, R.Y. Tsien, Geneically encoded fluorescent reporters of protein kinase activities in living cells, Proc. Natl. Acad. Sci. U. S. A. 98 (2001) 15003–15008.
[25] M. Sato, T. Ozawa, K. Inukai, T. Asano, Y. Umezawa, Fluorescent indicators for imaging protein phosphorylation in single living cells, Nat. Biotechnol. 20 (2002) 287–294.
[26] J.D. Violin, J. Zhang, R.Y. Tsien, A.C. Newton, A genetically encoded fluorescent reporter reveals oscillatory phosphorylation by protein kinase C, J. Cell Biol. 161 (2003) 899–909.
[27] K. Truong, M. Ikura, The use of FRET imaging microscopy to detect protein–protein interactions and protein conformational changes in vivo, Curr. Opin. Struck. Biol. 11 (2001) 573–578.
[28] L. Tyas, V.A. Brophy, A. Pope, A.J. Rivett, J.M. Tavaré, Rapid caspase-3 activation during apoptosis revealed using fluorescence-resonance energy transfer, EMBO Rep. 1 (2000) 266–270.
[29] M. Rehm, H. Düßmann, R.U. Jänicke, J.M. Tavaré, D. Kögel, J.H.M. Prehn, Single-cell fluorescence resonance energy transfer analysis demonstrates that caspase activation during apoptosis is a rapid process: role of caspase-3, J. Biol. Chem. 277 2002, pp. 24506–24514.
[30] K.Q. Luo, V.C. Yu, Y. Pu, D.C. Chang, Application of the fluorescence resonance energy transfer method for studying the dynamics of caspase-3 activation during UV-induced apoptosis in living HeLa cells, Biochem. Biophys. Res. Commun. 283 (2001) 1054–1060.
[31] M.J. Morgan, A. Thorburn, Measurement of caspase activity in individual cells reveals differences in the kinetics of caspase activation between cells, Cell Death Differ. 8 (2001) 38–43.
[32] R. Ohnuki, A. Nagasaki, H. Kawasaki, T. Baba, T.Q.P. Uyeda, K. Taira, Confirmation by FRET in individual living cells of the absence of significant amyloid β-mediated caspase 8 activation, Proc. Natl. Acad. Sci. U. S. A. 99 (2002) 14716–14721.
[33] K. Takemoto, T. Nagai, A. Miyawaki, M. Miura, Spatio-temporal activation of caspase revealed by indicator that is insensitive to environmental effects, J. Cell Biol. 160 (2003) 235–243.
[34] K.Q. Luo, V.C. Yu, Y. Pu, D.C. Chang, Measuring dynamics of caspase-8 activation in a single living HeLa cell during TNFalpha-induced apoptosis, Biochem. Biophys. Res. Commun. 304 (2003) 217–222.
[35] T. Fernandes-Alnemri, G. Litwack, E.S. Alnemri, CPP32, a novel human apoptotic protein with homology to *Caenorhabditis elegans* cell death protein Ced-3 and mammalian interleukin-1 beta-converting enzyme, J. Biol. Chem. 269 (1994) 30761–30764.
[36] H. Suzuki, K. Uchida, H. Shima, T. Sato, T. Okamoto, T. Kimura, M. Miwa, Molecular cloning of cDNA for human poly(ADP-rybose) polymerase and expression of its gene during HL-60 cell differentiation, Biochem. Biophys. Res. Commun. 146 (1987) 403–409.
[37] R.C. Scaduto Jr., L.W. Grotyohann, Measurement of mitochondrial membrane potential using fluorescent rhodamine derivatives, Biophys. J. 76 (1999) 469–477.
[38] C.J. Donahue, M. Santoro, D. Hupe, J.M. Jones, B. Pollok, R. Heim, D. Giegel, Correlating cell cycle with apoptosis in a cell line expressing a tandem green fluorescent protein substrate specific for group II caspases, Cytometry 45 (2001) 225–234.
[39] F. Yamasaki, S. Hama, H. Yoshioka, Y. Kajiwara, K. Yahara, K. Sugiyama, Y. Heike, K. Arita, K. Kurisu, Staurosporine-induced apoptosis is independent of p16 and p21 and achieved via arrest at G2/M and at G1 in U251MG human glioma cell line, Cancer Chemother. Pharmacol. 51 (2003) 271–283.
[40] C.M. Luetjens, D. Kögel, C. Reimertz, H. Dübmann, A. Renz, K. Schulze-Osthoff, A.-L. Nieminen, M. Poppe, J.H.M. Prehn, Multiple kinetics of mitochondrial cytochrome *c* release in drug-induced apoptosis, Mol. Pharmacol. 60 (2001) 1008–1019.
[41] H. Düssmann, D. Kögel, M. Rehm, J.H.M. Prehn, Mitochondrial membrane permeabilization and superoxide production during apoptosis: a single-cell analysis, J. Biol. Chem. 278 (2003) 12645–12649.
[42] M.L.R. Lim, M.-G. Lum, T.M. Hansen, X. Roucou, P. Nagley, On the release of cytochrome *c* from mitochondria during cell death signaling, J. Biomed. Sci. 9 (2002) 488–506.
[43] J.C. Goldstein, N.J. Waterhouse, P. Juin, G.I. Evan, D.R. Green, The coordinate release of cytochrome *c* during apoptosis is rapid, complete and kinetically invariant, Nat. Cell Biol. 2 (2000) 156–162.
[44] M. Madesh, B. Antonsson, S.M. Srinivasula, E.S. Alenemri, G. Hajnóczky, Rapid kinetics of tBid-induced cytochrome *c* and Smac/DIABLO release and mitochondrial depolarization, J. Biol. Chem. 277 (2002) 5651–5659.
[45] F. De Giorgi, L. Lartigue, M.K.A. Baure, A. Schubert, S. Grimm, G.T. Hanson, S.J. Remington, R.J. Youle, F. Ichas, The permeability transition pore signals apoptosis by directing Bax translocation and multimerization, FASEB J. 16 (2002) 607–609.